Effects of the nozzle arrangement and aerator configuration in slug bubble production to enhance the foulant removal from a flat sheet membrane bioreactor

Nazila Sutudehnezhad[1], Amir Heydarinasab[1], Reza Yegani[2,3*], Farshid Pajoum Shariati[1]

[1]Department of Chemical Engineering, Science and Research Branch, Islamic Azad University, Tehran, Iran
[2]Faculty of Chemical Engineering, Sahand University of Technology, Tabriz, Iran
[3]Membrane Technology Research Center, Sahand University of Technology, Tabriz, Iran

ABSTRACT

Membrane bioreactors (MBRs) are high-tech systems for water recycling and reusing of unconventional water resources such as municipal wastewater. However, the fouling of polymeric membranes is the main impediment to the market development of MBR. The polyolefin-based membranes are subjected to more severe organic fouling than other hydrophilic membranes due to their inherent strong hydrophobic properties, therefore, proposing efficient, fast, and economic fouling mitigation methods is vital for durable and long-standing performance. In this research, the hydrodynamics of a lab-scale membrane bioreactor with different configurations of aerators and nozzle sizes were used to investigate the air scouring efficiency. It was gained that aerators with higher air flow rates, e.g., 5.5 m/s can produce slug bubbles which are capable of foulant removal from the membrane surface. In comparison with a non-central aerator, the satisfactory scouring zone of the central aerator is narrow and the edge nozzles on both sides of the aerator are blocked. Under constant air flow rate, when the inlet air is injected into the aerator from two and three points, not only the end nozzles are blocked but also the liquid is penetrated into the aerator and the shear stress on the membrane surface decreased to 0.765 Pa. In the case of the non-central aerator, the satisfactory scouring zone becomes wider and neither nozzle blockage nor liquid penetration down to the aerator has occurred. The distribution of bubbles was optically evaluated by video imaging through the transparent plexiglass tank using aerators with different inlet flow rates and various configurations. Numerical simulations and related experimental analyses demonstrated that air inlet velocity has an important role in creating larger slug bubbles. It was shown that a non-central aerator in which the central nozzle in front of the inlet air stream is blocked, produces slug bubbles and sufficient air scoring on the flat sheet membrane. Configuration of a non-central aerator with 4 nozzles not only increased the satisfactory zone of each aerator without blockage of edge nozzles and liquid penetration into the aerator but also provided a higher shear rate over 1.104 Pa under a constant flow rate, which consequently removed the foulant from the membrane surface. **Polyolefins J (2023) 10: 117-126**

Keywords: Computational fluid dynamics; aerator; shear stress; satisfactory area; nozzle arrangement.

INTRODUCTION

Water scarcity is one of the most important matters and pressing challenges for people living in arid and semi-arid areas, such as water-deprived areas of the world. The deficiency of conventional water resources is exaggerated by population growth as well as the increase in irrigation and domestic water demand, which is difficult to be supplied from accessible natural resources [1]. Depending on the region and the availability of unconventional water resources consisting of seawater, municipal and industrial wastewater, and underground brackish water have been considered as potential substitute resources to supply the required water. Wastewater treatment is faced with several challenges consisting of energy consumption, operation difficulties and people skills,

Effects of the nozzle arrangement and aerator configuration in slug bubble production to enhance the foulant removal from a flat sheet....

IPPI

sludge management, footprint, and facilities [2]. The safe reuse of treated municipal wastewater for industrial and agricultural irrigation strongly depends on the selected wastewater treatment method. According to the literature [3-5], conventional wastewater treatment followed by an efficient polishing process, e.g., membrane filtration is promising to supply safe water. Membrane bioreactors (MBRs) is a smart, efficient, and attractive combination of conventional wastewater treatment and membrane filtration polishing step due to their small footprint which exists for several decades but has not yet overcome the market due to some drastic disadvantages such as membrane fouling [6].

Hydrophilic nanoparticle decorated polymer membranes show excellent performance to avoid organic and biological fouling compared to other conventional polyolefin-based membranes. However, the requirement for higher capital investment, the complexity of membrane manufacturing and its durable performance, and the requirement for very skilled operators are the main drawbacks that resist against their public utilization. Therefore, polyethylene and polypropylene polyolefin membranes are promising candidates to be used in the manufacturing of economically viable MBR. Due to the absence of any active functional group on the polyolefin polymers, dispersion, as well as uniform distribution of antifoulant nanoparticles, is a challenging issue, therefore, introducing of easy and efficient fouling mitigation method for polyolefin-based polymer membrane utilized in MBR system is the key point. Fouling removal is usually carried out using several techniques consisting of cleaning in place (CIP), backwashing processes, air blowing, membrane materials modification, and membrane module design [7, 8]. According to the literature, air scouring has been considered as the most effective, smooth, cost-effective method to mitigate the foulants from the membrane surfaces alongside with providing of dissolved oxygen for biomass growth.

Hydrodynamic conditions close to the membrane surface have a significant role in control of fouling. Air diffusing has been broadly used in submerged membrane bioreactor (SMBR) processes, and the aeration process design impacts the bubble formation process and accordingly influences the primary bubble distribution after production, so numerous aeration patterns have

been developed to facilitate the hydrodynamic impact in flat sheet membrane bioreactors (FSMBR) [9-12]. The aeration process of fine bubbles in comparison of slug bubble produced by large bubble aeration systems makes higher average shear stress in flat sheet membrane module [13-16]. The published reports on the impact of slug bubbling stated that the large bubbles could intensify surface shear, provide impressive control of concentration polarization and therefore improve membrane fouling [17-19]. Design characteristics of aerators, containing nozzle arrangement and length of aerator, impact the degree of non-monotony of bubbles made from different nozzles [20]. However, improvement and optimization of air diffusers and designing effective air nozzles according to practical experiences is a tedious, very time-consuming, and expensive procedure. On the other hand, computational fluid dynamics (CFD) which is an affordable method, can contribute to the understanding and prediction of properties of MBR. CFD is a numerical technique for mockup that can provide an optimization tool for predicting the effect of reactor design characteristics on the performance and hydrodynamics of the system. Most numerical researches have focused on the motion of slug bubbles along hollow fiber or tubular membrane modules and have been utilized to model time-based conversion in the three-dimensional changes of shear as a function of channel dimension, bubble size, and geometry for Newtonian fluids [13, 20].

Flows encountered in the MBR system are a mixture of various phases. Since the mixed liquor and activated sludge contains suspended solids and microorganisms, therefore in the presence of air bubbles it can be considered as a solid, liquid and gas multi-phase flow. Due to the very small size of microorganism, two phase models were widely considered in practical application and used in the simulations of multi-phase flow in MBRs [21]. In this case, the concept of volumetric fraction of each phase is introduced into these models, and the sum of the volumetric fraction of all phases should be equal to unity. Generally, three multi-phase models are available: the Eulerian model, the Mixture model, and the VOF model [22].

Among three abovementioned methods, the VOF approach enables to capture the interface of two or more immiscible fluids by tracking the volume fraction

of each phase in each computation cell throughout the domain. As this method is capable of tracking the motion of bubbles in water [23, 24], it makes possible to observe the bubbles' behavior and motion in aerated membrane modules, to develop novel aeration pattern [25, 26], to compare bubbly flow and slug flow [25-28], and to investigate the effect of bubble shape and trajectory [23, 24, 29-33].

The objectives of this paper are thus to investigate the influence of the aerator configuration including the effect of the air velocity in the inlet of the aerator and the impact of nozzles arrangement on the wall shear stress made by slug bubbles to study the hydrodynamic impacts on the FSMBR performance using the CFD simulation. In this work, the exerted surface shear stress in different aerator configurations and nozzle arrangements was analyzed and the satisfactory area of the slug bubble scouring zone was determined at an equal volumetric air flow rate to achieve more uniform distribution and enhanced membrane surface shear stress. The influence of flow rate on the formation of slug bubbles as well as the impact of the single/multiple air entries to the nozzles was also investigated. In this work, the nozzle arrangement and layout as well as the air inlet position in order to provide the sufficient scouring capability without nozzle blockage and fluid penetration into the nozzle holes were also investigated. Simulation results were finally validated by experimental data.

EXPERIMENTAL

Experimental setup
A lab-scale flat sheet MBR with a working volume of 2 L was prepared. Two flat sheet (FS) membrane modules with the dimensions of 51 × 10 × 4 mm (Length × Height × Thickness) were manufactured and fixed in the middle of the MBR tank that made by a transparent plexiglass sheet with the dimensions of 100 × 200 × 100 mm (Length × Height × Thickness). The distance between two flat sheet membrane modules was 10 mm. The aerator was placed between two FS membrane modules in the bottom of the tank, as shown in Figure 1.

To enable the imaging and clear observation of bubbles rising inside the flat sheet modules (FSM), one of the flat sheet modules was replaced by a transparent

Figure 1. Schematic view of membrane bioreactor.

plexiglass sheet with the same dimensions [26]. To generate slug bubbly flow, an aerator with nozzle diameter of 5 mm, and a distance between nozzle of 2 mm in two different inlet air velocities of 1.5 and 5.5 m/s, was prepared and used. The air flow rate was supplied by a HALEA ACO-5505 air blower and flow rate was measured and controlled using a HOEIBA-STEC -VP-2 soap film flow meter.

The MBR tank was filled with deionized water. Compressed air was supplied using an air blower to the liquid. The bubbling process was detected and documented by a high-speed A7S III Sony Camera with 4K resolution. All tests were repeated three times and directed at room temperature.

Simulation procedure
Modeling and meshing conditions
The characterization of hydrodynamic condition to form slug bubble was conducted using computational fluid dynamics (CFD) method. Various computational condition and domains were established on the basis of different geometries via GAMBIT 2.4.6 software. A tetrahedron-dominated mesh with an average mesh size of 1 mm was created for the aeration box as well as the flow region above the aerator to enhance the local tenacity to take the gas-liquid interface. The grid-independence improved grid used in the current study was about 2,035,675 elements with the min-max

Effects of the nozzle arrangement and aerator configuration in slug bubble production to enhance the foulant removal from a flat sheet....

IPPI

element sizes of 0.05-3 mm, respectively.

Governing equations
Three dimensional simulations were carried out using ANSYS FLUENT 2020. Considering several multiphase approaches which have been used to model the aeration process, the VOF (Volume of Fluid) model was utilized to determine the bubble movement in the liquid phase by considering an extra volume fraction equation [34]. The simulation was conducted by simultaneous solving of the momentum and mass conservation equations, and additional equations for interface and turbulence tracking procedure.

The continuity equation (mass balance) for incompressible two-phase flow is represented by the following equation:

$$\frac{\partial \rho}{\partial t} + \nabla(\rho \vec{u}) = 0 \tag{1}$$

and the momentum conservation equation is denoted as the following equation:

$$\frac{\partial}{\partial t}(\rho \vec{u}) + \nabla(\rho \vec{u}\vec{u}) = -\nabla p + \rho \vec{g} + \rho \vec{F} + \nabla \vec{\tau} \tag{2}$$

where u is the flow velocity, ρ is the volume-averaged density, p is the pressure, $\vec{F}$ and $\rho \vec{g}$ are the external body and gravitational forces, respectively. The volume-averaged density ρ was determined using the following equation:

$$\rho = \alpha \rho_g + (1-\alpha)\rho_l \tag{3}$$

where α ranges between 0 and 1. When the cell is completely filled by the liquid phase it equals to 0 and when the cell is completely filled by the gas phase, it becomes unity. ρ_g and ρ_l are gas and liquid phase densities, respectively.

The applied surface tension on the interfaces of the gas and liquid impacts the momentum at cells consisting the abovementioned interfaces [35]. The continuum surface force (CSF) model presented by other works [36] was combined into the proposed CFD model to simulate the applied surface tension at the gas and liquid interface.

Effect of phase turbulency made by the bubbling

procedure was conducted through SST k-ω model [35], in which ω and k are the specific dissipation rate and turbulence kinetic energy, respectively. Consequently, two extra transport equations for k and should be resolved, illustrated here as Eqs. (4) and (5), respectively:

$$\frac{\partial}{\partial t}(\rho k) + \frac{\partial}{\partial x_i}(\rho k u_i) = \frac{\partial}{\partial x_j}\left(\Gamma_k \frac{\partial k}{\partial x_j}\right) + G_K - Y_K + S_K \tag{4}$$

$$\frac{\partial}{\partial t}(\rho \omega) + \frac{\partial}{\partial x_i}(\rho \omega u_i) = \frac{\partial}{\partial x_j}\left(\Gamma_\omega \frac{\partial \omega}{\partial x_j}\right) + G_\omega - Y_\omega + D_\omega + S_\omega \tag{5}$$

In these equations, the terms G_K and G_ω signify the production of turbulence kinetic energy and the generation of turbulence kinetic energy due to the mean velocity gradients and buoyancy, respectively. Γ_K and Γ_ω represent the effective diffusivity of k and ω, respectively, which were computed as defined below.

$$\Gamma_k = \mu + \frac{\mu_t}{\sigma_k} \tag{6}$$

$$\Gamma_\omega = \mu + \frac{\mu_t}{\sigma_\omega} \tag{7}$$

The turbulent Prandtl numbers for *k* and *ω* were described with σ_k and σ_ω, respectively. The turbulent viscosity, μ_t was calculated as follows [37, 38]:

$$\mu_t = \frac{\rho k}{\omega} \frac{1}{\max\left[\frac{1}{\alpha^*}, \frac{SF_2}{\alpha_1 \omega}\right]} \tag{8}$$

The strain rate magnitude (S) and α^* were computed by:

$$\alpha^* = \alpha_\infty^*\left(\frac{\alpha_0^* + Re_t/R_k}{1 + Re_t/R_k}\right) \tag{9}$$

where

$$\alpha_\infty^* = 1 \tag{10}$$

$$Re_t = \frac{\rho k}{\mu \omega} \tag{11}$$

$$R_k = 6 \tag{12}$$

$$\alpha_0^* = \frac{\beta_i}{3} \ \& \ \beta_i = 0.072 \tag{13}$$

Boundary and Initial conditions
The membrane surface walls of the tank and floor were set as a no-slip wall for the liquid phase and a free-slip wall for the gas phase. Top of the computational network was set as a pressure outlet [34]. The inlet of the aerator was set as the velocity inlet. The initial flow velocity for both the liquid and air phases was applied as 0.

Numerical methods
All simulations were accomplished as transient performed on a pressure-based solver. Also, Geo-reconstruction method, the QUICK scheme and Second Order Upwind scheme were selected to resolve, volume fraction, the momentum, and turbulent kinetic energy equations, respectively. PISO was adopted for pressure-velocity coupling. PRESTO scheme was used for the pressure term discretization. All the simulations were performed in ANSYS FLUENT® 2020 with a 64-bit server (Intel® Core™ 12 Xeon CPU E5649) and 32 GB memory, running at a clock speed of 2.53 GHz. The total duration time for the process was defined to be 3 s. A time-step of 0.00001 s was used.

RESULTS AND DISCUSSION

Bubble production process and model validation
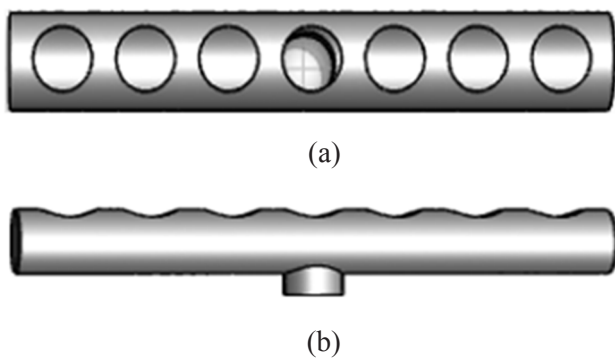The core of the conceptual context of the bubble producing process is the production and subsequent

Figure 2. Configuration of central inline aerator with 7 nozzles with a diameter of 5 mm, distance between nozzle of 2 mm, and 1 inlet of aerator; (a) upper view, (b) side view.
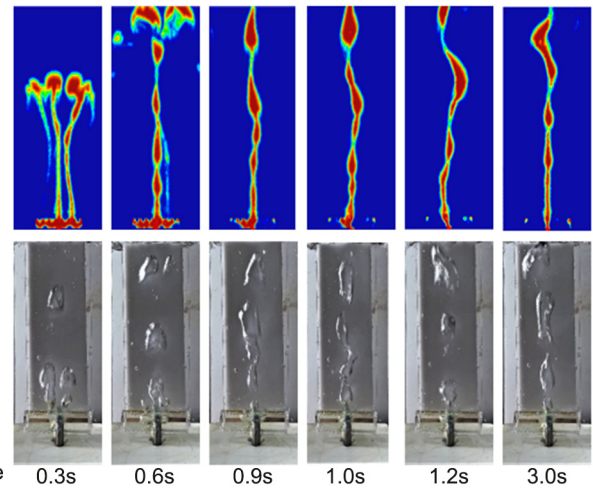

Figure 3. Experimental validation of central inline aerator with 7 nozzles with diameter of 5 mm, distance between nozzle of 2 mm, and 1 air inlet at different time intervals from 0.3 s to 3 s at an inlet velocity of 1.5 m/s.

distribution of bubbles into the membrane modules as the main influential parameters in hydrodynamic analyses of MBR performance. The utilized preliminary aerator configuration in this study is shown in Figure 2.

In order to form slug bubble, it is necessary to use aerator with bigger nozzle at higher inlet velocity [39]. According to the conducted CFD analysis shown in Figures 3 and 4, it can be seen that at low inlet air velocity equal to 1.5 m/s, the slug bubbles cannot be formed successfully, because inlet air cannot push up the liquid due to the static pressure caused by the fluid weight above the aerator; therefore, it results in
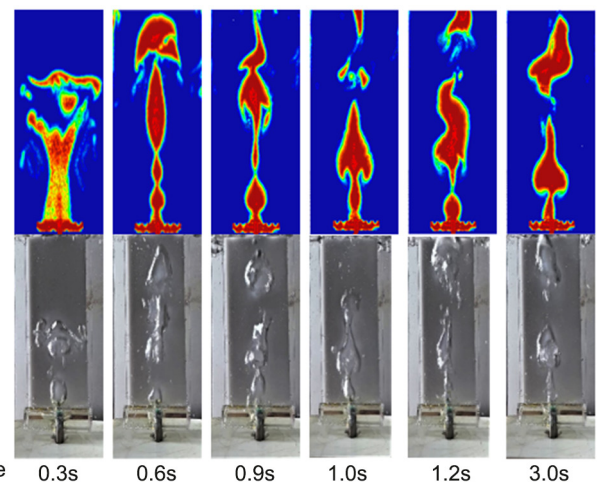

Figure 4. Experimental validation of central inline aerator with 7 nozzles with diameter of 5 mm, distance between nozzle of 2 mm, and 1 air inlet at different time intervals from 0.3 s to 3 s at an air inlet of 5.5 m/s.

Table 1. Average bubble-induced shear stress on the membrane surface in central inline aerator with 7 nozzles with a diameter of 5 mm, and distance between nozzle of 2 mm at different inlet air velocities.

Inlet air velocity (m/s)	Shear stress on the membrane surface (Pa)
1.5	0.274
5.5	0.951

blocking the nozzles and causes the fluid penetration into the aerator. In case of the central inline aerator, only one nozzle exerted bubbles into the membrane channels. Despite the larger diameter of the aerator nozzles, the lower velocity of the aerator inlet air resulted in production of small/medium bubbles and no slug bubble were observed. With increasing the air velocity from 1.5 to 5.5 m/s, it can be seen that the distribution of the air inside the aerator becomes somewhat uniform and prevents the fluid penetration into the aerator. However, although the slug bubbles are formed and scour the membrane surface, two nozzles located at the edge sides of the aerator were blocked and bubble were released from the middle nozzles shown in Figure 4. In this configuration, the satisfactory zone of slug bubbles was limited between three central nozzles. Although the edge nozzles were blocked due to the static pressure, however, liquid penetration did not occur. The determined shear stress was about 0.951 Pa.

Table 1 shows the amount of induced shear stress on the membrane surface. The obtained results show that the induced shear on the membrane surface increases when the inlet air velocity increases in aerator, which in turn, improves the hydrodynamics of the system and, as a result, reduces the amount of fouling on the
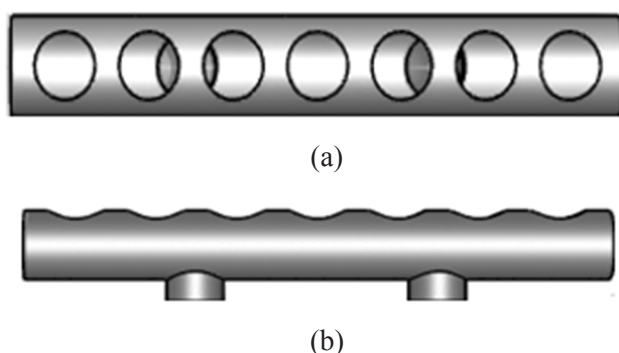

Figure 6. Air volume fraction contours from CFD prediction of aerator with 7 nozzles with diameter of 5 mm, distance between nozzle of 2 mm, and 2 inlets at different time intervals from 0.3 s to 3 s at a total air inlet velocity of 5.5 m/s.

membrane surface.

In order to investigate the impact of aerator configuration on the slug bubble satisfactory zone, inlet air was injected to the aerator from two and three entrances as shown in Figures 5 and 7, respectively at an overall constant flow rate.

Simulation results showed that when inlet air from two points, each with half flow rate was injected to the aerator, the satisfactory zone of slug bubbles was limited between three central nozzles. Similar to the single entry, the edge nozzles were blocked due to the static pressure and liquid penetration was not observed but the shear stress decreased to 0.851 Pa. Figure 6 shows air volume fraction contours from CFD prediction of aerator with 7 nozzles with diameter of 5 mm, distance between nozzle of 2 mm, and 2 inlets at different time interval from 0.3 s to 3 s at a total air inlet velocity of 5.5 m/s.

When the inlet air was injected through three points, similar to the previous configurations, the satisfactory zone of slug bubbles again was limited between three central nozzles and not only the edge nozzles were blocked, but also the liquid was penetrated into the

(a)

(b)

Figure 5. Configuration of aerator with 7 nozzles with diameter of 5 mm, and distance between nozzle of 2 mm, and 2 inlets of aerator; upper view (a), side view (b).
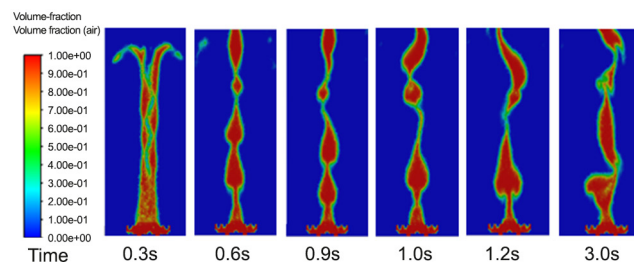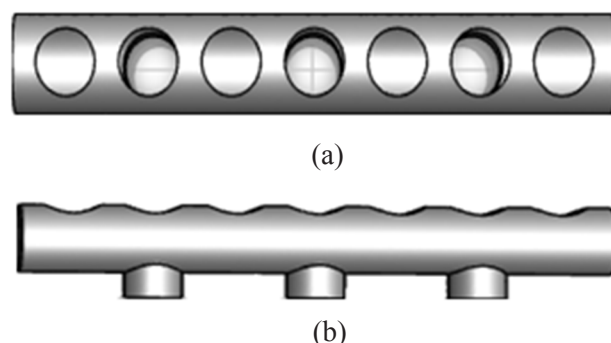

(a)

(b)

Figure 7. Configuration of aerator with 7 nozzles with diameter of 5 mm, and distance between nozzle of 2 mm and 3 inlets of aerator; (a) upper view, (b) side view.
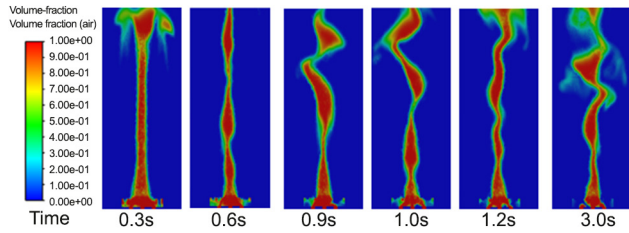
Figure 8. Air volume fraction contours from CFD prediction of aerator with 7 nozzles with diameter of 5 mm, distance between nozzle of 2 mm, and 3 inlets at different time intervals from 0.3 s to 3 s at a total air inlet velocity of 5.5 m/s.

Figure 10. Air volume fraction contours from CFD prediction of non-central aerator with 6 nozzles with a diameter of 5 mm and distance between nozzle of 2 mm, and 1 inlet at different time intervals from 0.3 s to 3 s at an air inlet velocity of 5.5 m/s.

aerator and the exerted shear stress decreased to 0.765 Pa. Figure 8 illustrates air volume fraction contours from CFD prediction of aerator with 7 nozzles with diameter of 5 mm, distance between nozzle of 2 mm, and 3 inlets at different time intervals from 0.3 s to 3 s at a total air inlet velocity of 5.5 m/s.

The results obtained confirmed that the satisfactory area of the slug bubbles is limited when a central inline aerator is utilized. Considering 7 nozzles on each aerator, the efficient length of each aerator is restricted to the three nozzles at a constant overall inlet air flow rate. Since our goal is to increase the satisfactory zone of each aerator without blockage of edge nozzles and liquid penetration into the aerator, non-central aerator was selected where the central nozzle located in front of the aerator inlet was sealed and the number of total nozzles on the aerator was decreased to 6. Figure 9 shows configuration of non-central aerator with 6 nozzles.

The results obtained were promising, showing that at constant flow rate, the satisfactory area increased and covered the whole of the aerator. Interestingly, neither
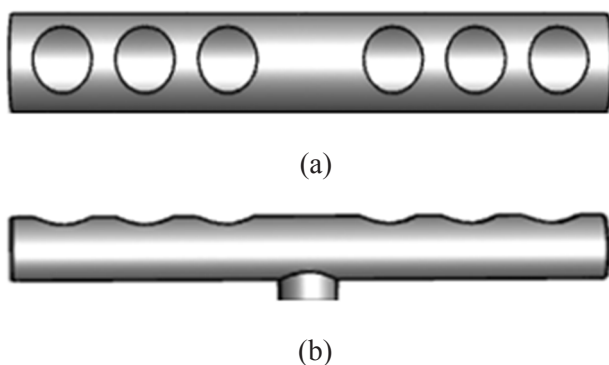
nozzle blockage, nor liquid penetration into the aerator occurred and the exerted shear stress increased to 1.033 Pa. The only drawback of the current configuration is the increase in the height of the appearance of slug bubbles along the flat sheet membrane module. Figure 10 demonstrates air volume fraction contours from CFD prediction of non-central aerator with 6 nozzles with diameter of 5 mm and distance between nozzle of 2 mm, and 1 inlet at different time intervals from 0.3 s to 3 s at an air inlet velocity of 5.5 m/s.

In order to shorten the height of slug bubble appearance along the membrane module, the end nozzle in each side was sealed and CFD simulation was conducted with the similar flow rate. Figure 11 shows the configuration of non-central aerator with 4 nozzles.

The results obtained represents that in this situation, the satisfactory area increased and the height of slug bubble appearance extended, corresponding to the better scouring capability due to the presence of slug bubbles and shear stress increment. Interestingly, neither nozzle blockage nor liquid penetration

(a)

(b)

Figure 9. Configuration of non-central aerator with 6 nozzles with diameter of 5 mm, and distance between nozzle of 2 mm, (a) upper view, (b) side view.
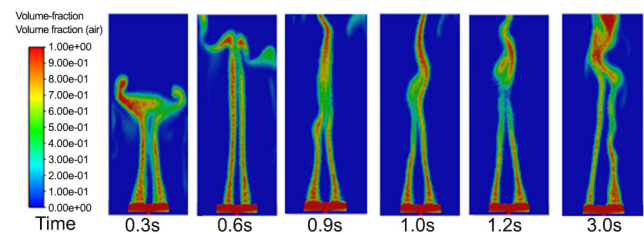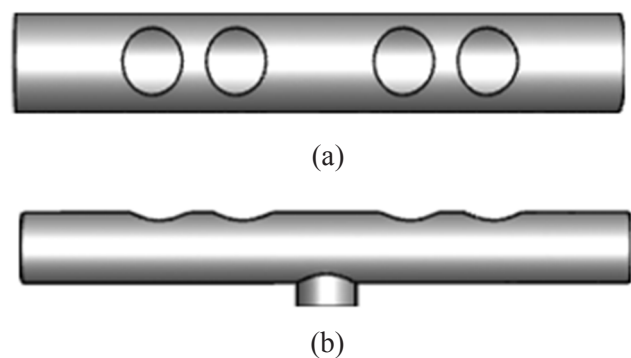

(a)

(b)

Figure 11. Configuration of non-central aerator with 4 nozzles with diameter of 5 mm, and distance between nozzle of 2 mm, (a) upper view, (b) side view.

Effects of the nozzle arrangement and aerator configuration in slug bubble production to enhance the foulant removal from a flat sheet....
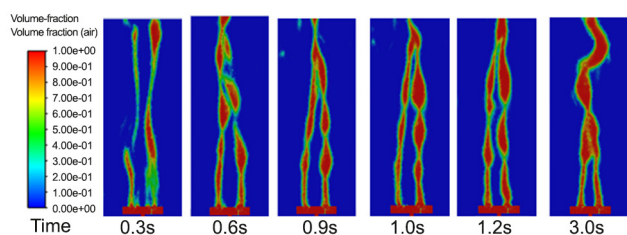
IPPI

Figure 12. Air volume fraction contours from CFD prediction of non-central aerator with 6 nozzles with diameter of 5 mm, and distance between nozzle of 2 mm, at different time intervals from 0.3 s to 3 s at an air inlet velocity of 5.5 m/s.
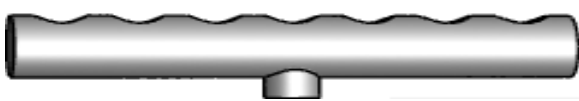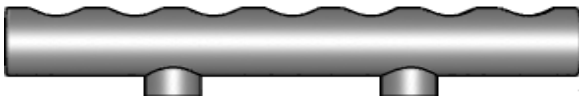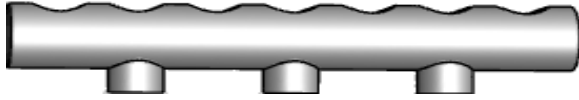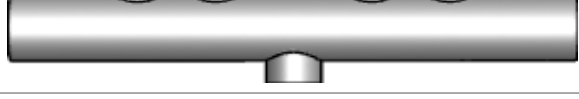
occurred, confirming that the current aeration strategy is sufficient and better performance is expected. The exerted shear stress increased to 1.104 Pa. Figure 12 shows air volume fraction contours from CFD prediction of non-central aerator with 4 nozzles with diameter of 5 mm, and distance between nozzle of 2 mm, at different time intervals from 0.3 s to 3 s at an air inlet velocity of 5.5 m/s.

induced shear stress on the membrane surface in different configurations of aerators at 5.5 m/s inlet air velocity. It can be understood that in the non-central aerator with 4 nozzles with diameter of 5 mm, and distance between nozzle of 2 mm induced shear stress on the membrane surface in comparison of the other aerators is higher.

CONCLUSION

In this work, the applied shear stress on the membrane surface in different aerator configurations and nozzle arrangements was investigated using CFD simulation and experimental setup under equal volumetric air flow rate. The influence of flow rate on the formation of slug bubbles as well as the impact of the single/ multiple air entries to the nozzles was also investigated. In this work, the nozzle arrangement and layout as well as the air inlet position in order to provide the sufficient scouring capability without nozzle blockage and fluid penetration into the nozzle holes were also investigated. Simulation results were finally validated by experimental data. The obtained results confirmed that the induced shear on the membrane surface increases with increasing the inlet air velocity in aerator and reduces the amount of fouling on the membrane surface. In comparison to the practical method, the optimization of the chemical process and fluid flow using computational fluid dynamic accompanied by experimental results is an efficient and time-saving method. Despite of the difficulties and complexity of CFD simulation in the membrane bioreactor system which requires approximate and near-certain assumptions as well as practical experiences, it is very effective, fast, and reliable method that gives deep insight to the complex flow patterns. The results

Table 2. Average bubble-induced shear stress on the membrane surface in a different configuration of aerators at 5.5 m/s inlet air velocity.

Configuration of aerators	Shear stress on the membrane surface (Pa)
	0.951
	0.851
	0.765
	1.033
	1.104

obtained from CFD simulation after validation in lab scale MBRs can be easily promoted and scaled up to the practical application. In addition, it was shown that simple manipulation in aerator could give higher performance in foulant removal efficacy from flat sheet membrane bioreactor. This finding is promising for publicity and wider utilization of economically viable polyolefin-based polymer membranes e.g., polyethylene and polypropylene, due to their weak functionality and easy organic fouling.

CONFLICTS OF INTEREST

The authors declare that they have no conflicts of interest.

REFERENCES

1. Salehi M (2022) Global water shortage and potable water safety; today's concern and tomorrow's crisis. Environ Int 158: 106936

2. Sonune A, Ghate R (2004) Developments in wastewater treatment methods. Desalination 167: 55-63

3. Mohajerani M, Mehrvar M, Ein-Mozaffari F (2009) An overview of the integration of advanced oxidation technologies and other processes for water and wastewater treatment. Int J Eng 3: 120-146

4. Al-Qodah Z, Al-Qudah Y, Assirey E (2020) Combined biological wastewater treatment with electrocoagulation as a post-polishing process: A review. Separ Sci Technol 55: 2334-2352

5. Liew WL, Kassim MA, Muda K, Loh SK, Affam AC (2015) Conventional methods and emerging wastewater polishing technologies for palm oil mill effluent treatment: A review. J Environ Manage 149: 222-235

6. Judd S (2010) The MBR book: Principles and applications of membrane bioreactors for water and wastewater treatment. Ed., Elsevier

7. Gruskevica K, Mezule L (2021) Cleaning methods for ceramic ultrafiltration membranes affected by organic fouling. Membranes 11: 131

8. Cui Z, Wang J, Zhang H, Ngo HH, Jia H, Guo W, Gao F, Yang G, Kang D (2018) Investigation of backwashing effectiveness in membrane bioreactor (MBR) based on different membrane fouling stages. Biores Technol 269: 355-362

9. Field RW, Zhang K, Cui Z, Hwang B-K (2011) Flat sheet MBR: Analysis of TMP rise and surface mass transfer coefficient. Desalin Water Treat 35: 82-91

10. Li Q, Cui Z, Pepper D (1997) Effect of bubble size and frequency on the permeate flux of gas sparged ultrafiltration with tubular membranes. Chem Eng J 67: 71-75

11. Le-Clech P, Chen V, Fane TA (2006) Fouling in membrane bioreactors used in wastewater treatment. J Membr Sci 284: 17-53

12. Judd S, Le-Clech P, Taha T, Cui Z (2001) Theoretical and experimental representation of a submerged membrane bio-reactor system. Membr Technol 2001: 4-9

13. Khalili-Garakani A, Mehrnia MR, Mostoufi N, Sarrafzadeh MH (2011) Analyze and control fouling in an airlift membrane bioreactor: CFD simulation and experimental studies. Process Biochemistry 46: 1138-1145

14. Yamanoi I, Kageyama K (2010) Evaluation of bubble flow properties between flat sheet membranes in membrane bioreactor. J Membr Sci 360: 102-108

15. Braak E, Alliet M, Schetrite S, Albasi C (2011) Aeration and hydrodynamics in submerged membrane bioreactors. J Membr Sci 379: 1-18

16. De Temmerman L, Maere T, Temmink H, Zwijnenburg A, Nopens I (2015) The effect of fine bubble aeration intensity on membrane bioreactor sludge characteristics and fouling. Water Res 76: 99-109

17. Zhang K, Field R, Cui Z (2006) Measurement of the mass transfer coefficients in submerged flat sheet membrane systems. In: Hotel Naxos Beach Resort in Giardini Naxos, Taormina (Messina), Italy: The Conference of the European Membrane Society.

18. Ghosh R, Cui Z (1999) Mass transfer in gas-sparged ultrafiltration: Upward slug flow in

Effects of the nozzle arrangement and aerator configuration in slug bubble production to enhance the foulant removal from a flat sheet....

IPPI

tubular membranes. J Membr Sci 162: 91-102

19. Liao WC (1999) Flux enhancements in cross-flow microfiltration., The University of Tennessee

20. Du X, Liu X, Wang Y, Radaei E, Lian B, Leslie G, Li G, Liang H (2017) Particle deposition on flat sheet membranes under bubbly and slug flow aeration in coagulation-microfiltration process: Effects of particle characteristic and shear stress. J Membr Sci 541: 668-676

21. Christopher EB (2005) Fundamentals of multiphase flows. Cambridge University, Press UK

22. Ansys fluent, a documentation theory guide (2015)

23. Ratkovich N, Chan C, Berube PR, Nopens I (2009) Experimental study and CFD modelling of a two-phase slug flow for an airlift tubular membrane. Chem Eng Sci 64: 3576-3584

24. Taha T, Cui ZF (2006) CFD modelling of slug flow in vertical tubes. Chem Eng Sci 61: 676-687

25. Wang B, Zhang K, Field RW (2018) Novel aeration of a large-scale flat sheet MBR: A CFD and experimental investigation. AIChE J 64: 2721-2736

26. Wang B, Zhang K, Field RW (2018) Slug bubbling in flat sheet MBR: Hydrodynamic optimization of membrane design variables through computational and experimental studies. J Membr Sci 548: 165-175

27. Wei P, Zhang K, Gao W, Kong L, Field R (2013) CFD modeling of hydrodynamic characteristics of slug bubble flow in a flat sheet membrane bioreactor. J Membr Sci 445: 15-24

28. Javid SM, Passandideh-Fard M, Faezian A, Goharimanesh M (2017) Slug and bubble flows in a flat sheet ultrafiltration module: Experiments and numerical simulation. Int J Multip Flow 91: 39-50

29. Cui Z, Taha T (2003) Enhancement of ultrafiltration using gas sparging: A comparison of different membrane modules. J Chem Technol Biotechnol: 78: 249-253

30. Essemiani K, Ducom G, Cabassud C, Liné A (2001) Spherical cap bubbles in a flat sheet nanofiltration module: Experiments and numerical simulation. Chem Eng Sci 56: 6321-6327

31. Taha T, Cheong W, Field R, Cui Z (2006) Gas-sparged ultrafiltration using horizontal and inclined tubular membranes—A CFD study. J Membr Sci 279: 487-494

32. Drews A, Prieske H, Meyer E-L, Senger G, Kraume M (2010) Advantageous and detrimental effects of air sparging in membrane filtration: Bubble movement, exerted shear and particle classification. Desalination 250: 1083-1086

33. Yang J, Vedantam S, Spanjers H, Nopens I, Van Lier JB (2012) Analysis of mass transfer characteristics in a tubular membrane using CFD modeling. Water Res 46: 4705-4712

34. Dhotre M, Niceno B, Smith B (2008) Large eddy simulation of a bubble column using dynamic sub-grid scale model. Chem Eng J 136: 337-348

35. Fluent A (2013) Ansys fluent theory guide 15.0. ANSYS, Canonsburg, PA 33

36. Brackbill JU, Kothe DB, Zemach C (1992) A continuum method for modeling surface tension. J Comput Phys 100: 335-354

37. Matsson JE (2022) An introduction to ansys fluent 2022. Ed., SDC Publications

38. Reynolds W (1987) Fundamentals of turbulence for turbulence modeling and simulation, Stanford Univ CA Dept of Mechanical Engineering

39. Wang B, Zhang K, Field RW (2018) Optimization of aeration variables in a commercial large-scale flat-sheet MBR operated with slug bubbling. J Membr Sci 567: 181-190